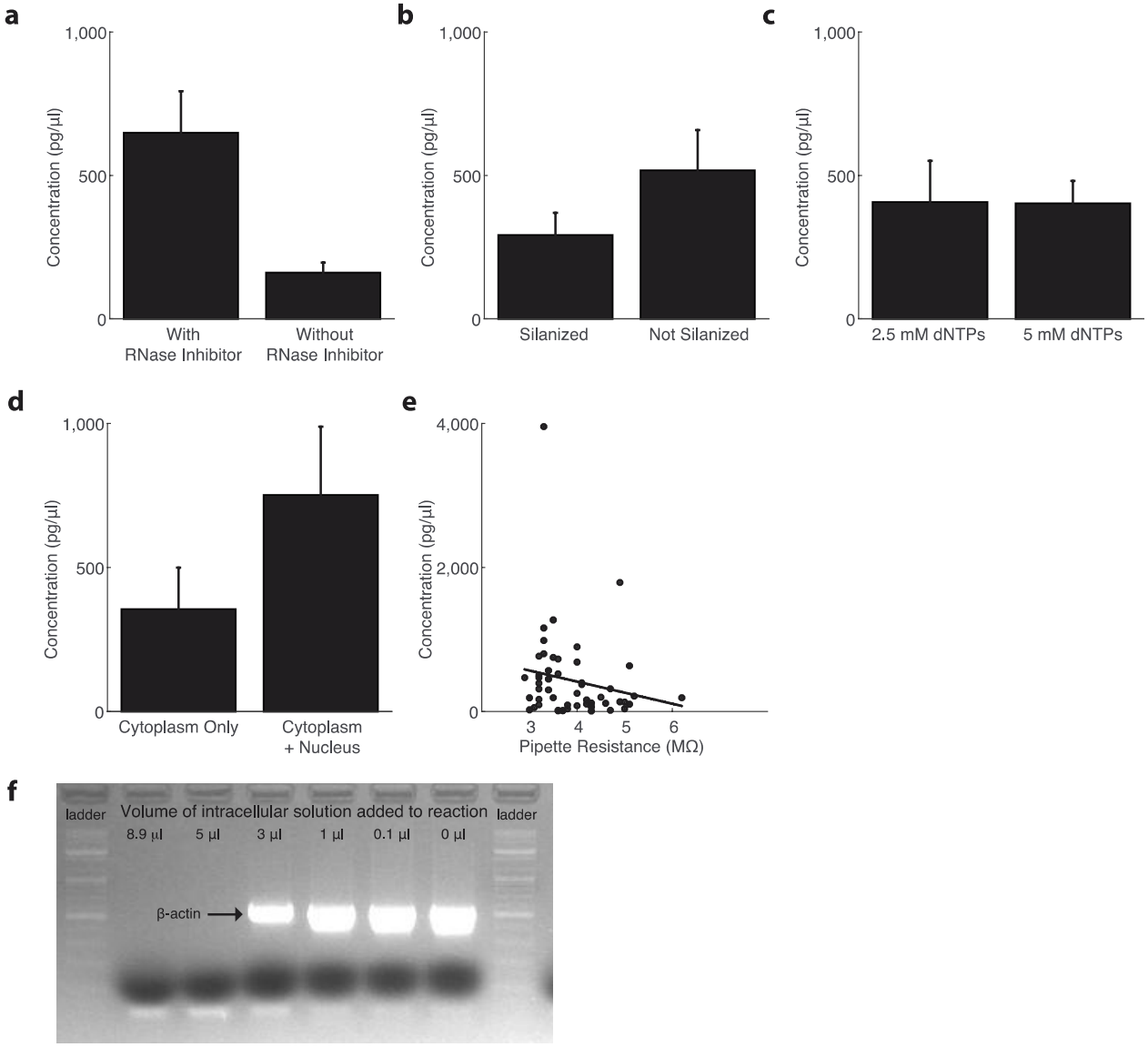

Supplementary Figure 1

Optimization of Patch-seq protocol.

Pilot experiments were carried out to test the effect of various protocol modifications on cDNA yield, including addition of RNase inhibitor to the intracellular solution **(a)**, silanization of glass capillaries **(b)**, concentration of dNTPs in lysis buffer **(c)**, extraction of cytoplasm only v. cytoplasm and nucleus **(d)**, pipette tip size **(e)** (tip size inversely proportional to resistance, line represents linear regression), and volume of intracellular solution in patch pipette (**f)** (20 µl total reaction volume, RT-PCR performed on whole brain cDNA template).

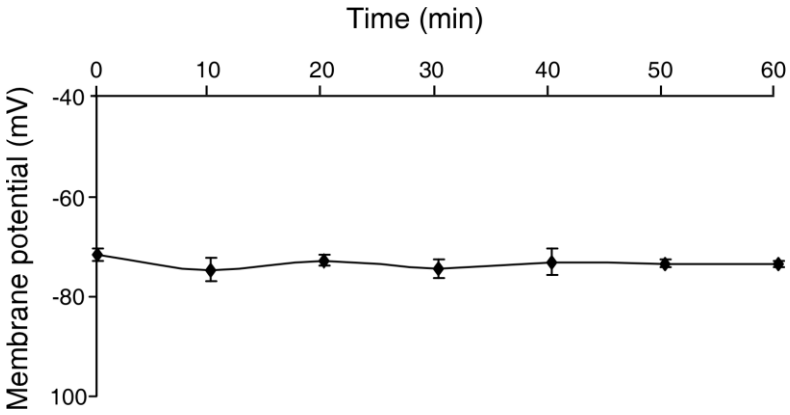

Supplementary Figure 2

Modified RNase-free intracellular solution does not affect health of patch-clamp-recorded neurons.

Membrane potential of neurons patched with RNase-free modified intracellular solution for Patch-seq recordings. Data represent mean ± SE (n=3 neurons).

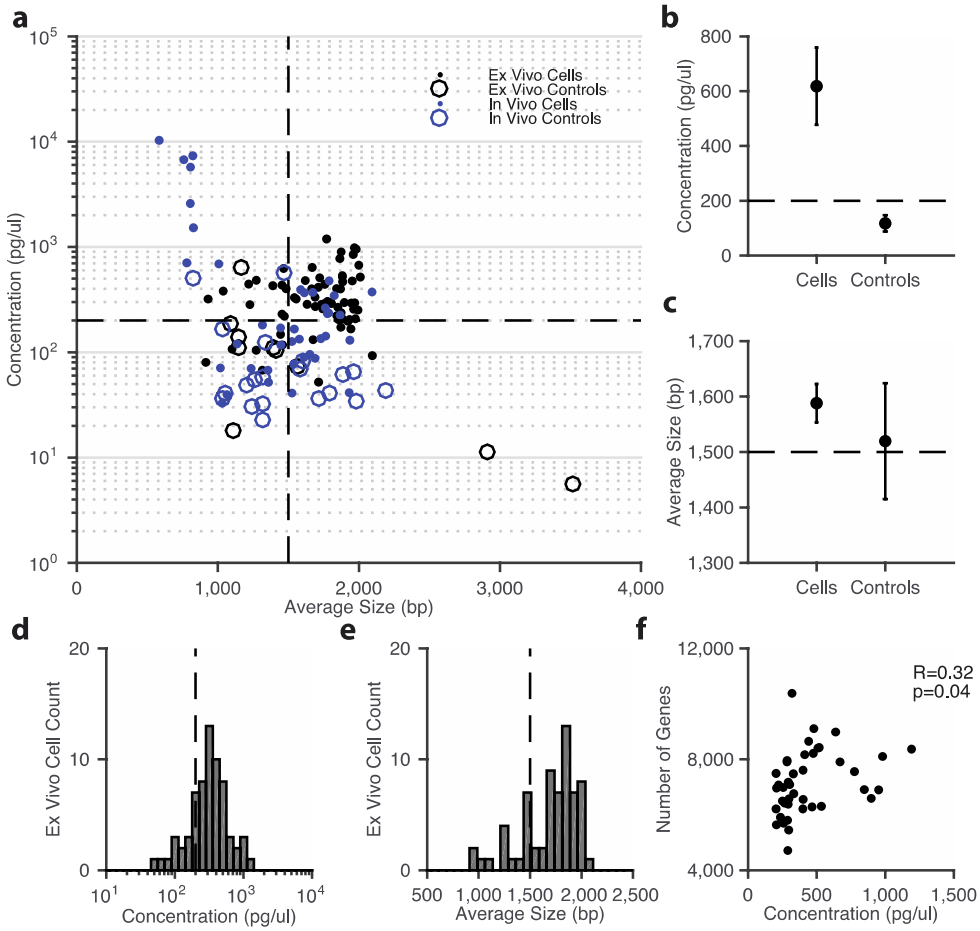

Supplementary Figure 3

Quality control of cDNA libraries.

(a) Average size and concentration (from 300-9,000 bp) of all collected samples. Only samples with more than 200 pg/µl and an average size greater than 1,500 bp were sequenced (criteria denoted by dashed lines). Libraries generated from patched cells generally contained more **(b)** and higher quality, full-length **(c)** cDNA compared to negative controls in which no cell was patched. Distributions of concentrations **(d)** and average sizes **(e)** of cDNA libraries generated from *ex vivo* patched cells. Dashed lines in (b-e**)** indicate threshold criteria used for sequencing. **(f)** Pearson correlation between concentration of cDNA and number of genes detected for all sequenced *ex vivo* cells.

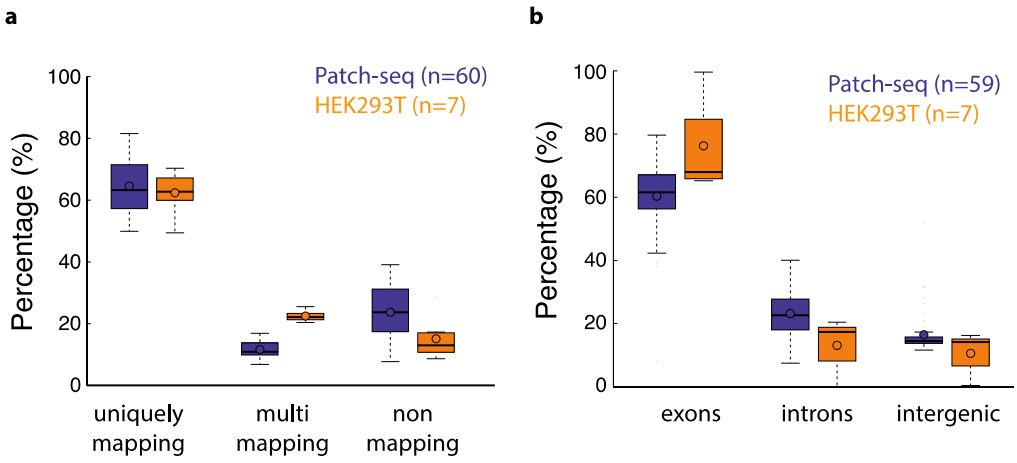

Supplementary Figure 4

Mapping statistics of Patch-seq and standard Smart-seq2 libraries.

(a) Percentage of sequenced reads that aligned uniquely to the respective assembly for patched single neurons and dissociated HEK293T cells picked and sequenced according to standard Smart-seq2 protocol (Picelli et al. 2013). **(b)** Percentage of uniquely aligned reads that overlap annotated RefSeq exons, introns or between gene annotations. This comparison indicates that the libraries generated from patched single neurons have similar qualities as standard Smart-seq2 libraries generated from lysed whole cells.

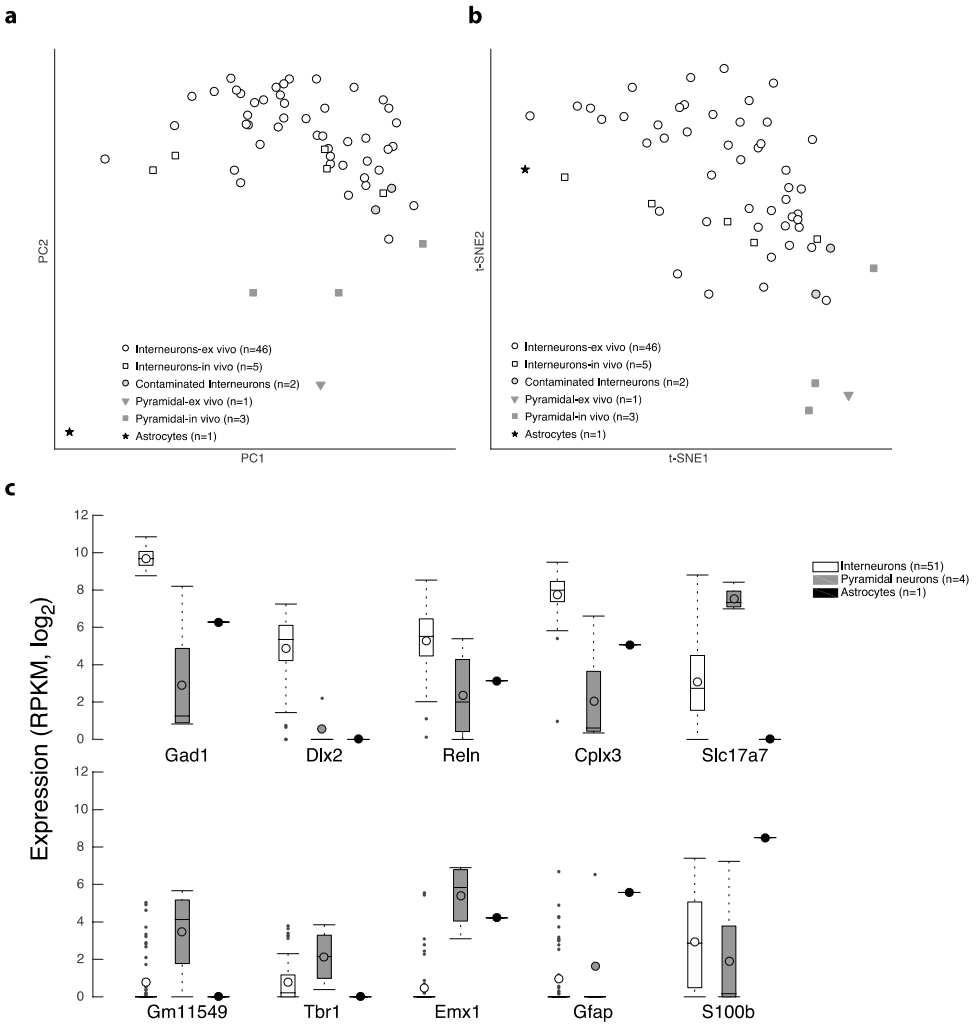

Supplementary Figure 5

Dimension reductions and marker expression in interneurons, pyramidal neurons and astrocyte.

(a) Principal component analyses (PCA) of the expression profiles of 16,000 genes detected in any of the patched cells. Each cell was projected onto a two-dimensional space drawn by the first two principal components. **(b)** Two-dimensional representation of cells using t-SNE on the PCA space, as in (a) but considering the first 28 principal components. Note that single outlier cells cannot be well captured in t-SNE representations as a consequence of the neighborhood analyses of the closest 20 cells (perplexity parameter). Therefore, the distinct gene expression observed in the astrocyte in the PCA (a) is not well captured in the t-SNE map. **(c)** Boxplots that show marker gene expression for interneurons, pyramidal neurons and the astrocyte. The mean and median are represented by the circle and black line, respectively. The edges of the box represent the 25th and 75th percentiles. Outlier cells are marked with grey dots, and the whiskers extend to extreme data points not considered outliers.

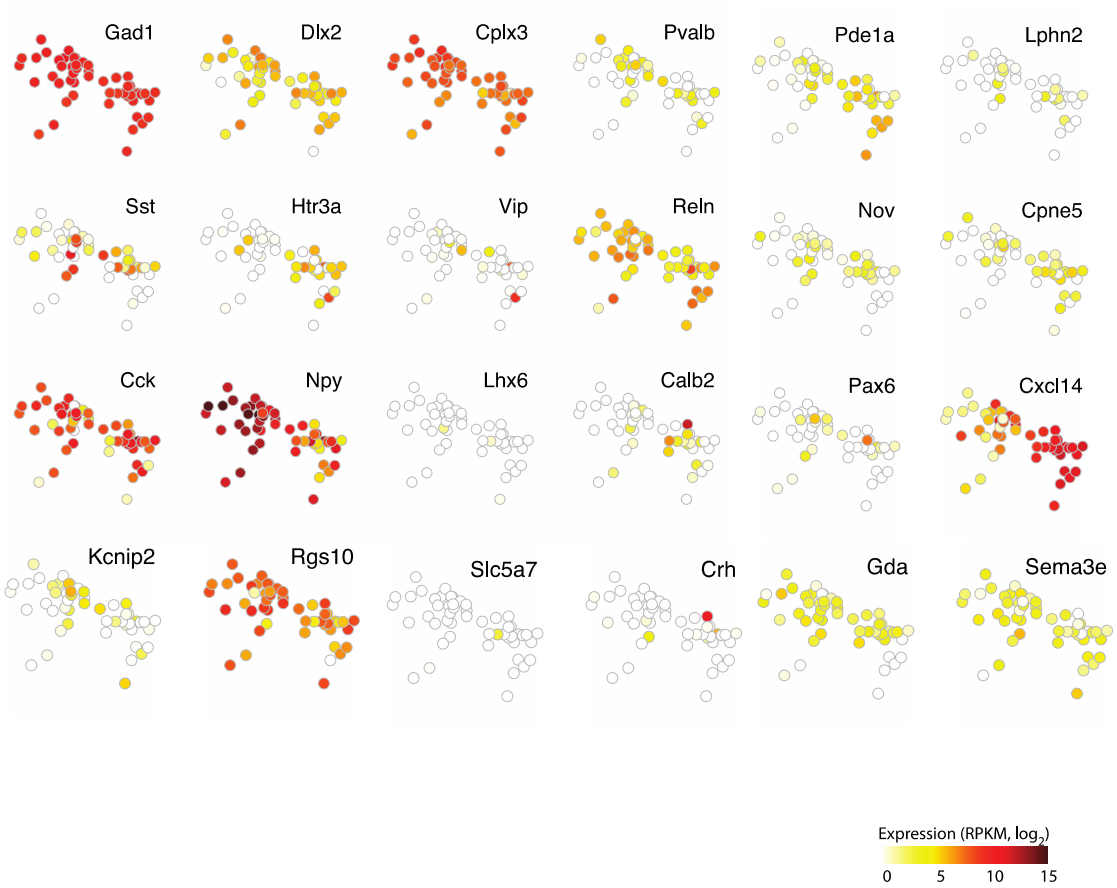

Supplementary Figure 6

Marker gene expression overlaid onto *t*-SNE map.

Marker gene expression overlaid onto the two-dimensional t-SNE representation (from Fig. 2d,e). Colors according to $\log_2$- transformed gene expression values.

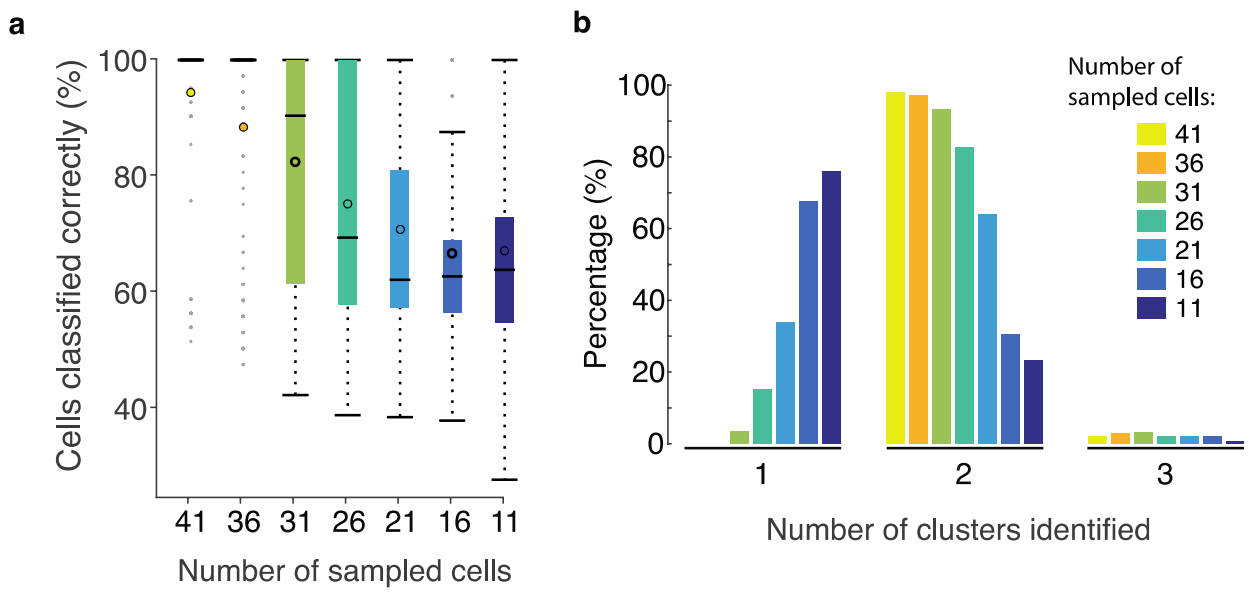

Supplementary Figure 7

Clustering of random samples of L1 interneurons.

Investigating the smallest number of patched cells needed to identify the two L1 interneuron cell types with unbiased clustering of gene expression profiles. **(a)** Affinity propagation was used to cluster random subsets of L1 interneurons (*ex vivo* cells, n=46) at decreasing numbers of cells. After each subsampling and clustering, the cell assignments were compared to the assignment based on all cells (Fig. 2d) and the accuracy score calculated (i.e. the number of correctly assigned cells over all subsampled cells). Accuracy scores from the 250 iterations per step are shown as standard boxplots, with median and mean as a line and circle, respectively. Importantly, even with random samples of 31 cells we robustly captured the two cell types (median accuracy=90%). Sampling fewer cells, in particular below 26 cells, often failed to distinguish the two cell types in an unbiased manner. **(b)** Showing the percentage of iterations where the affinity propagation clustering resulted in one, or two or three clusters, with the subsampling of decreasing numbers of L1 interneurons. The decline in performance at lower cell numbers was mainly caused by an inability of the affinity propagation algorithm to find two clusters, and instead reporting only one cluster.

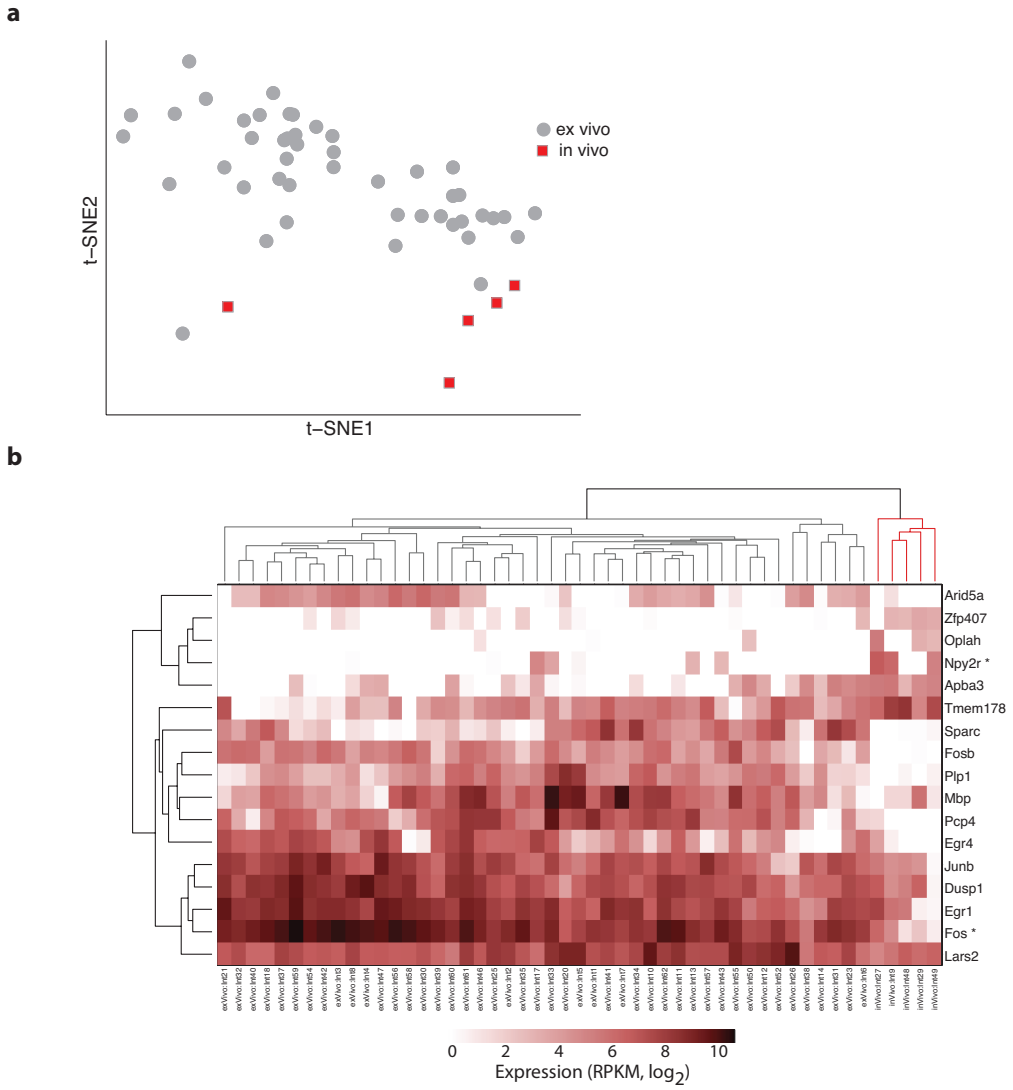

Supplementary Figure 8

Expression differences in interneurons patch-clamp-recorded *ex vivo* and *in vivo*.

(a) Coloring the t-SNE map (from Fig. 2d,e) according to *ex vivo* and *in vivo* patched neurons. **(b)** Heat map showing the top 17 genes that separate *ex vivo* and *in vivo* cells The genes were identified using SCDE and all have absolute values of Z-score above 1.96 (genes with asterisk have corrected absolute Z-score above 1.96). The heat map shows an increased expression of genes *ex vivo* relating to stress induction (including Fos, Fosb, Junb) and other genes with differential expression.

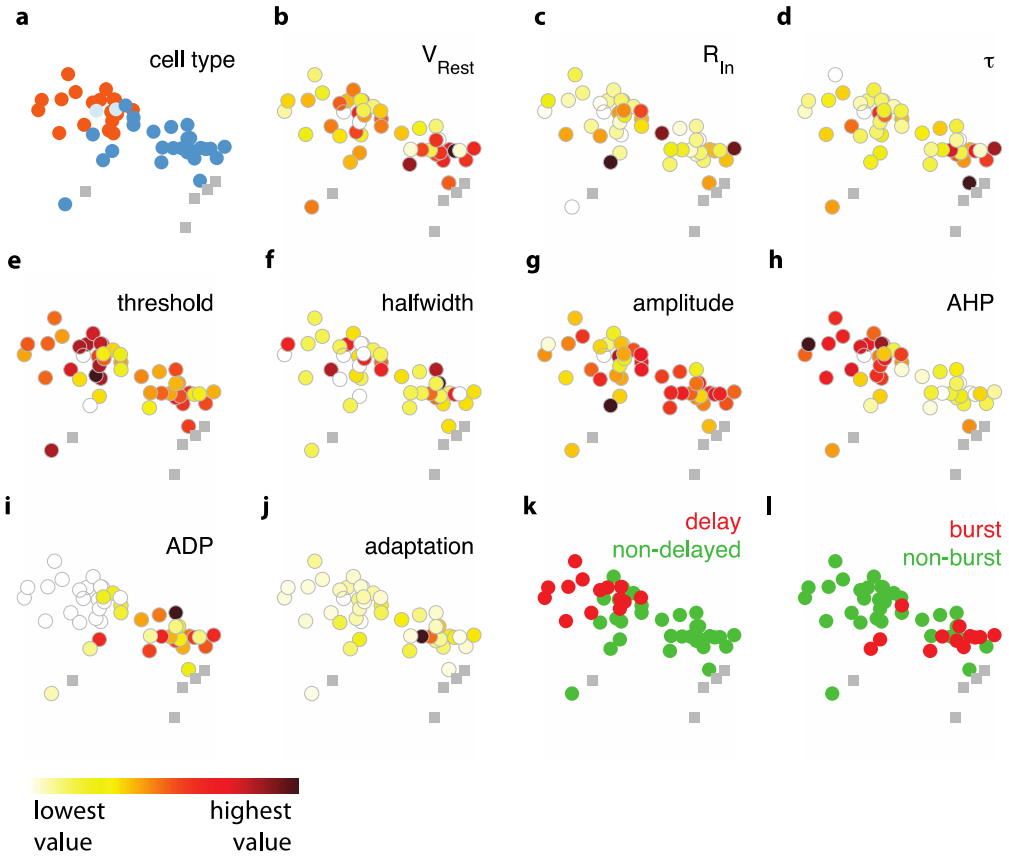

Supplementary Figure 9

Overlaying electrophysiological properties of cells onto the two-dimensional *t*-SNE map.

Coloring of cells in the t-SNE space according to their electrophysiological properties. **(a)** Identical to Fig. 2e, showing cell type assignments onto the t-SNE map, included to ease the comparison to panels b-l. **(b-j)** Cells colored according to continuous electrophysiological features, scaled by the highest and lowest measurement onto the indicated colorbar. **(k-l)** Cells colored based on their displayed spiking patterns during recordings. Grey squares show *in vivo* patched cells.